

Paradox resolved: stop signal race model with negative dependence

Hans Colonius^{a,c,1} and Adele Diederich^{b,1,2}

^aOldenburg University; ^bJacobs University Bremen

This manuscript was compiled on February 18, 2018

The ability to inhibit our responses voluntarily is an important case of cognitive control. The stop-signal paradigm is a popular tool to study response inhibition. Participants perform a response time task (*go task*) and, occasionally, the go stimulus is followed by a stop signal after a variable delay, indicating subjects to withhold their response (*stop task*). The main interest of modeling is in estimating the unobservable stop-signal processing time, that is, the covert latency of the stopping process as a characterization of the response inhibition mechanism. In the *independent race model* the stop-signal task is represented as a race between stochastically independent go and stop processes. Without making any specific distributional assumptions about the processing times, the model allows to estimate the mean time to cancel a response. However, neurophysiological studies on countermanding saccadic eye movements have shown that neural correlates of go and stop processes consist of networks of mutually *interacting* gaze-shifting and gaze-holding neurons. This poses a major challenge in formulating linking propositions between the behavioral and neural findings. Here we propose a *dependent race model* that postulates perfect negative stochastic dependence between go and stop activations. The model is consistent with the concept of interacting processes while retaining the simplicity and elegance of the distribution-free independent race model. For mean data, the dependent model's predictions remain identical to those of the independent model. The resolution of this apparent paradox advances the understanding of mechanisms of response inhibition and paves the way for modeling more complex situations.

response inhibition | stop signal paradigm | independent race model | perfect negative dependence

A recurrent theme in cognitive modeling is the difficulty to uniquely identify the processes underlying the generation of response times and probabilities in behavioral paradigms like simple yes-no tasks or same-different judgments of stimulus pairs. A prime example is the serial vs. parallel processing issue (1–3) showing that even rigorous mathematical analyses of the underlying assumptions may not always resolve the difficulty completely. Recently, efforts in model-based cognitive neuroscience to constrain behavioral models by findings obtained from neuroscientific methods have intensified, from spike train analyses to EEG and fMRI recordings (4). One area where important advances have emerged from this joint endeavor is the modeling of cognitive control and, in particular, response inhibition (5, 6). Response inhibition refers to the ability to suppress responses that are no longer required or have become inappropriate; it is important for survival, such as stopping yourself from crossing the street when a car comes around the corner without noticing you. Deficits of response inhibition have been linked to several disorders like attention-deficit/hyperactivity, obsessive-compulsive behavior and substance abuse. Probing response inhibition has been used widely to study executive control and flexibility in behavior; for reviews, see (6–9) and a recent theme issue of *Philosophical Transactions of the Royal Society B* (2017) on ‘Movement suppression: brain mechanisms for stopping and stillness’ (10)

In the laboratory, a very useful tool for the study of inhibition is the *stop-signal paradigm* where participants perform a response time task (*go task*), such as moving their gaze to the location of a pre-defined target. Occasionally, the go stimulus is followed by a stop signal after a variable time delay, indicating subjects to withhold the response (*stop task*). Performance in the stop-signal paradigm has been modeled as a race between a “go process”, triggered by the presentation of the go stimulus, and a “stop process” triggered by the presentation of the stop signal (6, 8). When the stop process finishes before the go process, the response is inhibited; otherwise, it is executed. The main interest of the modeler is in estimating the unobservable stop-signal reaction time (SSRT), that is, the latency of the stopping process as a characterization of the response inhibition mechanism. In the *independent race model* (IND model, for short) the stop-signal task is represented as a race between *stochastically independent* go and stop processes (11). Under certain simplifying assumptions, mean SSRT can be estimated efficiently without making any specific assumptions about the distribution of the processing times (6). In several hundreds of studies, the IND model has been applied in virtually every stop-signal experiment providing important measures of cognitive control like SSRT. Although the model makes no commitment to the underlying computational or neural processes that generate the go and stop processing times, the IND model is considered as defining constraints that any model of response inhibition must follow (12).

However, neurophysiological studies in the frontal eye fields (FEF) and superior colliculus (SC) of macaque monkeys performing a countermanding task with saccadic eye movements have shown that the neural correlates of go and stop processes produce eye movement behavior through a network of *interacting* gaze-shifting and gaze-holding neurons (13–16). This discrepancy between the behavioral and neural data is widely perceived as a paradox (9, 12, 17, 18): how can interacting circuits of mutually inhibitory neurons instantiate stop and go processes with stochastically independent finishing times?

Here we propose a variant of the race model which, instead of independence, assumes *perfect negative stochastic dependence* between go and stop processes (PND model, for short). It resolves the apparent paradox and nonetheless retains the distribution-free property of the independent race model. Moreover, the PND model's predictions, considered at the level of mean SSRT, are shown to be necessarily identical to those of the independent model. Notably, we argue that it is very difficult to empirically

125 distinguish between the two race model versions without introducing further, parametric assumptions. Thus, there is no reason 187
126 to uphold the stochastic independence assumption of the race model whenever a distribution-free version is to be considered. 188

127
128 **Neurally inspired modeling** 190

129 Investigating the neural underpinnings of response inhibition in saccades, Hanes and Schall (13) first showed that macaque 191
130 monkey behavior in saccade countermanding corresponded in detail to that of human performance in manual stop-signal tasks. 192
131 Then, recording from the frontal eye fields they isolated neurons involved in gaze-shifting and gaze-holding that represent 193
132 a larger circuit of such neurons that extends from cortex through basal ganglia and superior colliculus to brainstem (14). 194
133 Importantly, that result was based on their postulate that for neurons to participate in controlling movement initiation two 195
134 criteria must be met: first, neurons must discharge differently when movements are initiated or withheld; if neurons still 196
135 discharge when movements are canceled, their activity was not affected by the stop process. Second, the differential modulation 197
136 on canceled trials must occur before SSRT; otherwise, the neural modulation happens after the movement has already been 198
137 canceled (18, p.1012). From these findings, Boucher and colleagues (17) developed an *interactive race model* linking the 199
138 interacting circuits of mutually inhibitory gaze-holding and gaze-shifting neurons with stochastic accumulation in the go and 200
139 stop processes of the race model (see also 19). A response is observed only if the go process reaches a certain threshold of 201
140 activation. Stopping occurs if the stop process interferes with the go process by inhibiting activation in the go accumulator to 202
141 prevent it from reaching the threshold. Alternative models assume that response inhibition results from blocking the input to 203
142 the go unit (“blocked-input models”) (20) or postulate a spiking neural network of hundreds of units representing populations 204
143 of movement neurons, fixation neurons and inhibitory interneurons, and a control unit that turns the fixation neurons on and 205
144 off (21). 206

145 These neural models are computationally explicit: they are based on systems of stochastic differential equations; estimating 207
146 parameters to best fit the behavioral data, they are able to predict the distribution of cancel times, i.e., the times at which 208
147 neural activity modulates on trials on which subjects stop successfully, relative to SSRT (12). The models fit the behavioral 209
148 data just as well as the independent race model. Note that this is just another instantiation of the paradox. An attempt to 210
149 resolve the contradiction between stochastic independence for behavioral data and interdependence at the neural level has been 211
150 to postulate that the stop process is independent of the go process for much of its duration, followed by a late and potent 212
151 interaction between stopping and going that reverses the trajectory of go activation (12, 17). Strictly speaking, this would 213
152 require introducing two subsequent processing stages in the IND model, independence followed by strong interaction. No 214
153 formal modeling of this extension has been undertaken, however, to the best of our knowledge. 215

154
155 **Background: General race model** 217

156
157 Next, we present a formal framework for the general race model making no assumption at all about the dependency between 219
158 stop and go processes. One should distinguish between two different experimental conditions termed context \mathcal{GO} where only a 220
159 go signal is presented, and context \mathcal{STOP} where a stop signal is presented in addition. A race between processes triggered by 221
160 the go and stop signal is represented by two random variables: T_{go} and T_{stop} (referred to as SSRT above) denote the random 222
161 processing times for the go and stop signal, respectively, in context \mathcal{STOP} with a bivariate distribution function denoted H , 223

$$162 \quad H(s, t) = \Pr[T_{go} \leq s, T_{stop} \leq t], \quad [1] \quad 224$$

163 defined for all real numbers s and t , with $s, t \geq 0$. The marginal distributions of $H(s, t)$ are 225

$$164 \quad F_{go}(s) = \Pr[T_{go} \leq s, T_{stop} < \infty] \text{ and} \quad 226$$

$$165 \quad F_{stop}(t) = \Pr[T_{go} < \infty, T_{stop} \leq t]. \quad 227$$

166
167 In context \mathcal{STOP} the go signal triggers a realization of random variable T_{go} and the stop signal triggers a realization of random 230
168 variable T_{stop} . In context \mathcal{GO} , however, only processing of the go signal occurs. In general, the latter one may be different from 231
169 the marginal distribution $F_{go}(s)$ in context \mathcal{STOP} . However, the *general race model* rules this out by adding the important 232
170 assumption of “context invariance”, also know as “context independence” (e.g. 9): 233

171
172
173

174 Significance Statement 236

175
176 The ability to suppress a response that is no longer required or has become inappropriate is an important act of cognitive control. 238
177 Deficits in inhibiting a response to a stop signal have been linked to disorders like attention-deficit/hyperactivity. A widely accepted 239
178 model for the stop signal paradigm assumes that stop signal processing occurs independently from go signal processing and permits 240
179 to estimate the covert latency of the stop process. However, neurophysiological data suggest interactive neural networks of going 241
180 and stopping raising a contradiction between the behavioral and neural findings. Introducing a model with strong negative stochastic 242
181 dependency between go and stop processing resolves the paradox while retaining the computational simplicity of the original model. 243

182
183

184 Authors declare no conflict of interest. 245

185 ¹H.C. and A.D. contributed equally to this work. 246

186 ²To whom correspondence should be addressed. E-mail: hans.colonius@uni-oldenburg.de 247

249 **Context invariance (CI).** In context \mathcal{GO} , the distribution of go signal processing time is assumed to be 311
 250
$$F_{go}(s) = \Pr[T_{go} \leq s, T_{stop} < \infty],$$
 312 [2] 313
 251
 252 i.e., it is identical to the marginal distribution $F_{go}(s)$ in context \mathcal{STOP} . 314
 253 From these assumptions, the probability of observing a response to the go signal, given a stop signal is presented with delay 315
 254 t_d [ms] ($t_d \geq 0$) after the go signal, is defined by 316
 255
$$p_r(t_d) = \Pr[T_{go} < T_{stop} + t_d].$$
 317 [3] 318
 256 According to the model, the probability of observing a response to the go signal no later than time t , given the stop signal was 319
 257 presented with delay t_d , is given by (conditional) distribution function 320
 258
$$F_{sr}(t | t_d) = \Pr[T_{go} \leq t | T_{go} < T_{stop} + t_d],$$
 321 [4] 322
 259 known as *signal-response RT* distribution. 323
 260 The main interest in race modeling is to obtain information about the distribution of the unobservable stop signal processing 324
 261 time T_{stop} , or about some of its parameters, given sample estimates of $F_{go}(t)$, $F_{sr}(t | t_d)$, and $p_r(t_d)$. As observed in (11), 325
 262 letting stop signal delay t_d vary, the *inhibition function* $p_r(t_d)$ can be formally considered as the distribution function of a 326
 263 random variable, $T_d \equiv T_{go} - T_{stop}$, say. Then, 327
 264
$$E[T_d] = E[T_{go}] - E[T_{stop}],$$
 328 [5] 329
 265 with $E[\cdot]$ denoting expected value (mean) of a random variable. Solving for the estimate of $E[T_{stop}]$ immediately yields an 330
 266 estimate of the mean of the unobservable distribution of T_{stop} . It is well known that the reliability of this estimation method, 331
 267 known as the *mean method*, depends on how precise the inhibition function $p_r(t_d)$ and the mean of T_{go} are estimated (6, 9). 332
 268 Obtaining estimates of higher moments, or the entire distribution of T_{stop} , requires further non-parametric assumptions about 333
 269 the bivariate distribution $H(s, t)$. 334
 270
 271 **Independent vs. negatively dependent race model** 335
 272
 273 The most common version of the race model, as introduced by Logan & Cowan (11), postulates stochastic independence 336
 274 between T_{go} and T_{stop} : 337
 275 **Stochastic independence:** 338
 276
$$H(s, t) = \Pr[T_{go} \leq s] \times \Pr[T_{stop} \leq t] = F_{go}(s) \times F_{stop}(t),$$
 339
 277 for all s, t ($s, t \geq 0$). 340
 278 In addition to estimating the mean via Equation [5], an estimate of the variance of stop signal processing time is obtainable 341
 279 in the IND model from 342
 280
$$\text{Var}[T_{stop}] = \text{Var}[T_d] - \text{Var}[T_{go}],$$
 343 [6] 344
 281 due to assuming stochastic independence. Finally, it can be shown that the unobservable stop signal distribution function 345
 282 $F_{stop}(t)$ is expressible as a function of the observables $p_r(t_d)$, $f_{go}(t)$ and $F_{sr}(t | t_d)$ (see Methods section). 346
 283 In order to resolve the paradox described above, a race model with negative dependency between go and stop signal 347
 284 processing times is proposed next. We define a bivariate distribution function for T_{go} and T_{stop} exhibiting *perfect negative* 348
 285 *dependence* (see, e.g., 22) as follows : 349
 286 **Perfect negative stochastic dependence:** 350
 287
$$H^-(s, t) = \max\{F_{go}(s) + F_{stop}(t) - 1, 0\}.$$
 351 [7] 352
 288 for all s, t ($s, t \geq 0$). The marginal distributions of $H^-(s, t)$ are the same as before, that is, $F_{go}(s)$ and $F_{stop}(t)$. Note that this 353
 289 perfect negative stochastic dependence (PND) model is parameter-free just like the IND race model, that is, we do not assume 354
 290 some specific parametric distribution. It can be shown (see Methods) that then 355
 291
$$F_{stop}(T_{stop}) = 1 - F_{go}(T_{go})$$
 356 [8] 357
 292 holds “almost surely”, that is, with probability 1. Thus, for any F_{go} percentile we immediately obtain the corresponding F_{stop} 358
 293 percentile as complementary probability and vice versa, expressing perfect negative dependence between T_{go} and T_{stop} . The 359
 294 relation in Equation [8] is also interpretable as “ T_{stop} is (almost surely) a decreasing function of T_{go} ”. 360
 295 The PND model arguably constitutes the most direct implementation of the notion of “mutual inhibition” observed in 361
 296 neural data: any increase of inhibitory activity (speed-up of T_{stop}) elicits a corresponding decrease in “go” activity (slow-down 362
 297 of T_{go}) and vice versa. 363
 298 **Predictions from the PND race model.** We list some predictions from the PND race model (for further details, see Methods 364
 299 section): 365
 300 **Probability of stopping.** Under perfect negative dependence between T_{go} and T_{stop} , the probability of stopping $p_r(t_d)$ is an 366
 301 increasing function of t_d , as it should. 367
 302
 303
 304
 305
 306
 307
 308
 309
 310

373 **Signal-response RT distribution.** Signal-response RT distribution 435
374 436
375 $F_{sr}(t|t_d) = \Pr[T_{go} \leq t | T_{go} < T_{stop} + t_d]$, [4] 437
376 438
377 approaches the go signal distribution $F_{go}(t)$ with increasing stop signal delay t_d . Moreover, for varying values of t_d , $F_{sr}(t|t_d)$ 439
378 exhibits the “fan effect” typically found in empirical data and also predicted by the IND race model (6, 11). 440
379 To illustrate, Figure 1 presents the go signal distribution and signal-response RT distributions with different delay values t_d 441
380 for both the IND (dashed curves) and the PND race model (solid lines) assuming exponential distributions for T_{go} and T_{stop} . 442
381 While the exponential distribution lacks empirical support, it was chosen here just to illustrate quantitative differences between 443
382 the model versions. 444
383 An important feature of the PND model is suggested by Figure 1: each signal-response distribution $F_{sr}(t|t_d)$ crosses 1 at 445
384 a certain finite point t . It is shown below that this point is predictable from the observables $p_r(t_d)$ and $F_{go}(t)$. While this 446
385 “crossing” property is not shared by the IND model (because the “coupling” of T_{go} and T_{stop} as expressed in Equation (8) is 447
386 absent), the strength of this test will of course depend on the precision of estimates of $F_{sr}(t|t_d)$. 448
387 **Estimating moments of the T_{stop} distribution.** Given that the marginal distributions F_{go} and F_{stop} are the same under both 449
388 models, any estimates for $E[T_{stop}]$ based on the mean method (Eq. [5]) are necessarily identical for the IND and PND model. 450
389 However, for the variance we obtain 451
390 452
391
$$\text{Var}[T_{stop}] = \text{Var}[T_d] - \text{Var}[T_{go}] + 2 \text{Cov}[T_{go}, T_{stop}].$$
 [9] 453
392 454
393 As the covariance in the above equation is unknown, an estimate for the stop signal variance is no longer available under the 455
394 PND model. Nevertheless, given that $\text{Cov}[T_{go}, T_{stop}]$ is the most extreme negative covariance under any bivariate distribution 456
395 for T_{go} and T_{stop} (23), the PND model stop signal variance can never be larger than the one under independence. 457
396 458
397 **Discussion** 459
398 460
399 **Testing IND vs. PND race models.** Because stop signal processing times are not observable, empirical testing of non-parametric 461
400 stop signal race models is severely limited in general. In particular, both the IND and PND version of the race model can only 462
401 be tested in conjunction with context invariance (CI). Presuming CI is valid, the following predictions can be tested: (1) mean 463
402 signal-response RT should be faster than mean go signal RT; (2) mean signal-response RT should increase with stop signal 464
403 delay t_d ; and (3) both these tests are implied by the “fan” structure of the distribution functions permitting an additional 465
404 qualitative test of IND and PND race models. Because data not consistent with this “fan” structure would be evidence against 466
405 both the IND and PND model, obviously, none of these tests would allow us to distinguish between IND and PND. 467
406 By construction, the PND model has the same distribution for stop signal processing as the IND model; therefore, estimates 468
407 for mean SSRT, i.e., the expected value of stop signal processing, will be identical for either model as long as estimates are 469
408 based on the mean method. In a sense, this is good news because it implies that adopting perfect negative dependency between 470
409 go and stop signal processing does not invalidate previous SSRT estimates of all empirical studies employing the mean method. 471
410 Note that this holds as well for estimating SSRT via the *integration method*, another way to estimate SSRT. However, because 472
411 the integration method presumes stop signal processing time to be constant, the distinction between IND and PND model 473
412 becomes meaningless. 474
413 This leaves us with the shape of the family of signal-response distributions, that is, $F_{sr}(t|t_d)$ for varying values of t_d , as the 475
414 only potential means of distinguishing between the two models. Whether or not this “crossing” test that -as outlined above- 476
415 consists of checking the way in which the signal-response distributions approach their upper bound of 1, proves to be as visible 477
416 in real data compared to the exponential toy example (Figure 1) will depend on the specific, but unobservable, stop signal 478
417 distribution. 479
418 480
419 **Conclusion.** Several authors have stressed that the level of description provided by the race model is quite different from that 481
420 of neural models (17, 20): the independent race model is mute about the possible underlying mechanisms of response inhibition, 482
421 and its primary purpose is to provide a measure of stop signal processing time, which the model allows without having to 483
422 assume a specific distribution or estimate parameters. Nevertheless, it has been claimed that the independent race model 484
423 “captures the essence of computation and ...that it formulates the constraints that any model of response inhibition must follow” 485
424 (cf. 20, p.3). The race model with perfect negative dependence suggested here operates at the same level of generality and 486
425 yields the same measure of (mean) stop signal processing time but, importantly, resolves the paradox the independent model is 487
426 facing due to the neurophysiological findings. We conclude that the race model with perfect negative stochastic dependence is 488
427 a natural way to unify the observation of interacting circuits of mutually inhibitory gaze-holding and gaze-shifting neurons 489
428 with data on the behavioral level. 490
429 Beyond the simple stop signal task, several other forms of acts of control have been studied that pose an even greater 491
430 challenge for efforts to identify the underlying cognitive processes, such as switching tasks or shifting of attention (5). One 492
431 promising area is *selective stopping* where response inhibition is required for some stimuli (e.g. red light) but not others (green 493
432 light) (e.g., 24). Representing cognitive processes for such more complex tasks may call for types of graded, instead of perfect, 494
433 dependency. Appropriate race models can easily be introduced by appealing to more general forms of stochastic dependency 495
434 via copulas (22). 496

497 **Methods** 559

498 This section presents some computational details for both the IND and PND model, in general and for the special case of 560
 499 exponential distributions (for producing Figure 1). 561

500 We assume that distribution functions F_{go} and F_{stop} possess densities, f_{go} and f_{stop} , and are increasing, where “increasing” 562
 501 always refers to “strictly increasing” here. Note that although it is usually taken for granted in the race model that densities 563
 502 exist, strictly speaking, this is not required neither by the independent nor the dependent race model. 564
 503 565

504 **Independent race model.** Under stochastic independence of T_{go} and T_{stop} , 566

$$\begin{aligned}
 p_r(t_d) &= \Pr[T_{go} < T_{stop} + t_d] \\
 &= \int_0^\infty f_{go}(t)[1 - F_{stop}(t - t_d)] dt.
 \end{aligned}
 \tag{10}$$

509 Moreover, 571

$$\text{Var}[T_d] = \text{Var}[T_{stop}] + \text{Var}[T_{go}],
 \tag{11}$$

511 implying Equation [6]. 572

512 Writing $f_{sr}(t | t_d)$ for the density function of signal-response time distribution $F_{sr}(t | t_d)$, it has been shown in (25) that 573
 513 574

$$f_{sr}(t | t_d) = f_{go}(t) [1 - F_{stop}(t - t_d)] / p_r(t_d).
 \tag{12}$$

514 From that, an explicit expression of the distribution of the unobservable stop signal processing time T_{stop} is given by: 575
 515 576
 516 577

$$F_{stop}(t - t_d) = 1 - \frac{f_{sr}(t | t_d)p_r(t_d)}{f_{go}(t)}.
 \tag{13}$$

519 Unfortunately, as investigated in (26, 27), gaining reliable estimates for the stop signal distribution using Equation [13] requires 581
 520 unrealistically large numbers of observations. 582
 521 583

522 **Perfect negative dependent race model.** Defining the bivariate distribution by 584

$$H^-(s, t) = \max\{F_{go}(s) + F_{stop}(t) - 1, 0\}
 \tag{7}$$

523 for all s, t ($s, t \geq 0$), the marginal distributions of $H^-(s, t)$ are again $F_{go}(s)$ and $F_{stop}(t)$. A classic result from the *theory of* 585
 524 *copulas* (see SI) asserts that 586
 525 587

526 (i) H^- is the lower bound of all bivariate distributions H of (T_{go}, T_{stop}) , i.e., $H^-(s, t) \leq H(s, t)$ for all (s, t) ; 588
 527 589

528 (ii) $\Pr[F_{go}(T_{go}) + F_{stop}(T_{stop}) = 1] = 1$. 590
 529 591

530 From (i) the covariance between the random variables can be shown to be the smallest possible across all bivariate distributions 592
 531 $H(s, t)$ (23). Statement (ii) is equivalent to 593

$$F_{stop}(T_{stop}) = 1 - F_{go}(T_{go}).
 \tag{8}$$

532 holding almost surely. 594
 533 595

534 **Probability of stopping.** Under perfect negative dependence between T_{go} and T_{stop} , 596
 535 597

$$\begin{aligned}
 p_r(t_d) &= \Pr[T_{go} - T_{stop} < t_d] \\
 &= \Pr[T_{go} - F_{stop}^{-1}[1 - F_{go}(T_{go})] < t_d] \\
 &= \Pr[g(T_{go}) < t_d] \\
 &= \Pr[T_{go} < g^{-1}(t_d)],
 \end{aligned}
 \tag{14}$$

536 where function g , defined as $g(t) = t - F_{stop}^{-1}[1 - F_{go}(t)]$, is increasing and so its inverse g^{-1} is increasing as well. Thus, $p_r(t_d)$ 604
 537 is increasing in t_d . 605
 538 606

539 **Signal-response RT distribution.** For stop signal delay t_d , 607

$$\begin{aligned}
 F_{sr}(t | t_d) &= \Pr[T_{go} \leq t | T_{go} < T_{stop} + t_d] \\
 &= \Pr[T_{go} \leq t \cap T_{go} < T_{stop} + t_d] / p_r(t_d) \\
 &= \Pr[T_{go} \leq t \cap T_{go} < g^{-1}(t_d)] / \Pr[T_{go} < g^{-1}(t_d)] \\
 &= F_{go}(\min\{t, g^{-1}(t_d)\}) / F_{go}(g^{-1}(t_d)).
 \end{aligned}$$

542 To see that $F_{sr}(t | t_d)$ obeys the “fan effect” consider two different delays, t_d and t_d^* , say, with $t_d < t_d^*$; for a fixed value of t , we 613
 543 first assume $t < g^{-1}(t_d) < g^{-1}(t_d^*)$. Then 614
 544 615

$$\begin{aligned}
 F_{sr}(t | t_d^*) &= F_{go}(t) / F_{go}(g^{-1}(t_d^*)) \\
 &< F_{go}(t) / F_{go}(g^{-1}(t_d)) \\
 &= F_{sr}(t | t_d).
 \end{aligned}$$

545 616
 546 617
 547 618
 548 619
 549 620
 550 The cases $g^{-1}(t_d) < t < g^{-1}(t_d^*)$ and $g^{-1}(t_d) < g^{-1}(t_d^*) < t$ can be shown similarly.

621 **Expected stop signal processing time.** A formal expression for mean (expected) stop signal processing time is obtained as follows. 683
 622 We have 684

$$\begin{aligned} E[T_{stop}] &= \int_0^\infty [1 - F_{stop}(s)] ds & 685 \\ &= \int_\infty^0 F_{go}(t) \frac{ds}{dt} dt \quad (\text{a.s.}), & 686 \end{aligned} \tag{15}$$

626 687
 627 688
 628 689
 629 using Equation [8] and the fact that $1 - F_{stop}(s)$ and $F_{go}(t)$ have opposite limit values. With 691
 630 692

$$s = F_{stop}^{-1}[1 - F_{go}(t)] \tag{15}$$

631 693
 632 694
 633 we have 695

$$\frac{ds}{dt} = -f_{go}(t)/f_{stop} [F_{stop}^{-1}[1 - F_{go}(t)]] . \tag{15}$$

634 696
 635 697
 636 698
 637 Inserting into [15] yields 699

$$E[T_{stop}] = \int_0^\infty \frac{F_{go}(t) f_{go}(t)}{f_{stop} [F_{stop}^{-1}[1 - F_{go}(t)]]} dt. \tag{16}$$

638 700
 639 701
 640 702
 641 **IND model: exponential case.** Define independent, exponential distributions for T_{go} and T_{stop} with parameters $\lambda_{go} > 0$ and 703
 642 $\lambda_{stop} > 0$ for context *STOP* by 704

$$\begin{aligned} H(s, t) &= \Pr[T_{go} \leq s] \times \Pr[T_{stop} \leq t] & 705 \\ &= (1 - \exp[-\lambda_{go} s]) \times (1 - \exp[-\lambda_{stop} t]), & 706 \end{aligned}$$

643 707
 644 708
 645 709
 646 710
 647 for all $s, t \geq 0$. Then 711

$$\begin{aligned} p_r(t_d) &= \int_0^{t_d} f_{go}(t) dt + \int_{t_d}^\infty f_{go}(t) [1 - F_{stop}(t - t_d)] dt & 712 \\ &= 1 - \frac{\lambda_{stop}}{\lambda_{stop} + \lambda_{go}} \exp[-\lambda_{go} t_d]. & 713 \end{aligned} \tag{17}$$

648 714
 649 715
 650 716
 651 717
 652 For $t > t_d$, the density of the signal-response distribution is given by, 718

$$\begin{aligned} f_{sr}(t | t_d) &= f_{go}(t) [1 - F_{stop}(t - t_d)] / p_r(t_d) & 719 \\ &= \frac{\lambda_{go} \exp[-\lambda_{go} t] \exp[-\lambda_{stop}(t - t_d)]}{\left(1 - \frac{\lambda_{stop}}{\lambda_{stop} + \lambda_{go}} \exp[-\lambda_{go} t_d]\right)} & 720 \\ &= \frac{1}{K} (\lambda_{go} + \lambda_{stop}) \exp[-(\lambda_{go} + \lambda_{stop})(t - t_d)], & 721 \end{aligned} \tag{18}$$

653 722
 654 723
 655 724
 656 725
 657 with $K = \exp[\lambda_{go} t_d] (1 + \lambda_{stop}/\lambda_{go}) - \lambda_{stop}/\lambda_{go}$. For $t_d = 0$, we have $K = 1$ and the signal-response density is identical to an 726
 658 exponential density for an independent race between T_{stop} and T_{go} , with parameter $\lambda_{go} + \lambda_{stop}$ and $p_r(t_d) = \lambda_{go}/(\lambda_{go} + \lambda_{stop})$. 727
 659 For $t \leq t_d$, the density simplifies to 728

$$\begin{aligned} f_{sr}(t | t_d) &= f_{go}(t) / p_r(t_d) & 729 \\ &= \frac{1}{\lambda_{stop} + \lambda_{go}} \exp[-\lambda_{go}(t - t_d)]. & 730 \end{aligned} \tag{19}$$

660 731
 661 732
 662 733
 663 734
 664 Computation of the expected value of signal-response RTs yields: 735

$$\begin{aligned} E[T_{go} | T_{go} < T_{stop} + t_d] &= \int_0^\infty t f_{sr}(t | t_d) dt & 736 \\ &= \frac{\lambda_{go} [1 + (\lambda_{go} + \lambda_{stop}) t_d]}{(\lambda_{go} + \lambda_{stop}) \{ \exp[\lambda_{go} t_d] (\lambda_{go} + \lambda_{stop}) - \lambda_{stop} \}}. & 737 \end{aligned} \tag{20}$$

665 738
 666 739
 667 740
 668 741
 669 742
 670 743
 671 744
 672 In particular, for $t_d = 0$, we obtain $E[T_{go} | T_{go} < T_{stop} + t_d] = 1/(\lambda_{go} + \lambda_{stop})$, consistent with the density we mentioned above
 673 for this value of the stop signal delay. 744

745 **PND model: exponential example.** Inserting exponential margins into the bivariate distribution,

$$\begin{aligned}
 H^-(s, t) &= \max\{F_{go}(s) + F_{stop}(t) - 1, 0\} \\
 &= \max\{1 - \exp[-\lambda_{go} s] - \exp[-\lambda_{stop} t], 0\},
 \end{aligned}
 \tag{21}$$

749 for all $s, t \geq 0$. From [14],

$$\begin{aligned}
 p_r(t_d) &= \Pr[T_{go} - T_{stop} < t_d] \\
 &= \Pr[T_{go} - F_{stop}^{-1}[1 - F_{go}(T_{go})] < t_d] \\
 &= \Pr[T_{go} - F_{stop}^{-1}[\exp(-\lambda_{go} T_{go})] < t_d] \\
 &= \Pr[T_{go} + 1/\lambda_{stop} \log[1 - \exp(-\lambda_{go} T_{go})] < t_d] \\
 &= \Pr[g(T_{go}) < t_d] \\
 &= \Pr[T_{go} < g^{-1}(t_d)].
 \end{aligned}
 \tag{22}$$

759 Note that function

$$g(T_{go}) \equiv T_{go} + 1/\lambda_{stop} \log[1 - \exp(-\lambda_{go} T_{go})]$$

762 cannot be solved explicitly for T_{go} . Therefore, in order to compute $p_r(t_d)$ and plot signal-response time distributions

$$F_{sr}(t | t_d) = F_{go}(\min\{t, g^{-1}(t_d)\})/F_{go}(g^{-1}(t_d)),$$

765 we sampled ($n = 100,000$) from the bivariate distribution function $H^-(s, t)$ using function **simCop** (based on the conditional simulation method, see (22)) from the **copBasic** package of the open source software R (<http://www.r-project.org>).

767 Table 1 lists the crossing points for the signal-response time distributions obtained from the simulation. They correspond to the vertical lines in Figure 1.

Table 1. Predictions for crossing points $F_{sr}(t | t_d) = 1.0$ in PND model

t_d [ms]	10	50	100	150
$g^{-1}(t_d)$	53.6	79.9	117.7	161.4

Compare with Figure 1

778 Supporting Information (SI)

780 **Fréchet-Hoeffding bounds and perfect dependency.** The dependence between two random variables of a random vector (X, Y) is completely described by its probability distribution. Let $G(x, y)$ be the bivariate distribution function of some random vector (X, Y) :

$$G(x, y) = P(X \leq x, Y \leq y)$$

784 with marginal distributions F_X and F_Y . Then, it always holds that

$$\begin{aligned}
 G^-(x, y) &= \max\{F_X(x) + F_Y(y) - 1, 0\} \leq G(x, y) \\
 &\leq \min\{F_X(x), F_Y(y)\} = G^+(x, y),
 \end{aligned}$$

789 for all x, y for which G is defined (the support of G). Both $G^-(x, y)$ and $G^+(x, y)$ are known as *Fréchet-Hoeffding bounds* and are themselves distribution functions for (X, Y) : G^- corresponds to “perfect” negative dependence between X and Y , while G^+ corresponds to “perfect” positive dependence (see (22) for proofs of this and other claims in this section). “Perfect” dependency can be formulated in various ways. For simplicity, we assume X and Y have continuous distribution functions, the only case we will need below. Here are three equivalent characterizations of *perfect negative dependence* (analogous results exist for perfect positive dependence, but they are not of concern here):

795 (i) Either $\Pr(X > x, Y > y) = 0$ for all x, y or

$$\Pr(X \leq x, Y \leq y) = 0 \text{ for all } x, y;$$

798 (ii) $\Pr[F_X(X) + F_Y(Y) = 1] = 1$;

800 (iii) X is almost surely a decreasing function of Y .

801 Consider the equation inside the “Pr” expression in (ii): Solving for X by taking the inverse function of $F_X(X)$ we get

$$X = F_X^{-1}[1 - F_Y(Y)],$$

805 from which (iii) follows. Random variables with perfect negative dependence are also known as *antithetic variates* in simulation studies.

869	1. D. Algom, A. Eidels, R.X.D. Hawkins, B. Jefferson, and J.T. Townsend. Features of response times: identification of cognitive mechanisms through mathematical modeling. In J.R. Busemeyer, Z. Wang, J.T. Townsend, and A. Eidels, editors, <i>The Oxford Handbook of Mathematical and Computational Psychology</i> , chapter 4, pages 63–98. Oxford University Press, New York, NY 10016, 2015. ISBN 9780199957996.	931
870		932
871	2. J.T. Townsend. Serial vs. parallel processing: Sometimes they look like tweedledum and tweedledee but they can (and should be) distinguished. <i>Psychological Science</i> , 1:46–54, 1990.	933
872	3. J.T. Townsend and M.J. Wenger. A theory of interactive parallel processing: new capacity measures and predictions for a response time inequality series. <i>Psychological Review</i> , 111(4):1003–1035, 2004.	934
873	4. B.U. Forstmann and E.J. Wagenmakers, editors. <i>An introduction to model-based cognitive neuroscience</i> . Springer-Verlag GmbH, New York Heidelberg Dordrecht London, 1st edition, 2015. ISBN 978-1-4939-2235-2. URL http://www.ebook.de/de/product/22860990/an_introduction_to_model_based_cognitive_neuroscience.html .	936
874	5. G.D. Logan. Takong control of cognition: an instance perspective on acts of control. <i>American Psychologist</i> , 72(9):875–884, 2017.	937
875	6. F. Verbruggen and G.D. Logan. Models of response inhibition in the stop-signal and stop-change paradigms. <i>Neuroscience & Biobehavioral Reviews</i> , 33:647–661, 2009. http://doi.org/10.1016/j.neubiorev.2008.08.014 .	938
876	7. G.D. Logan. On the ability to inhibit thought and action: A users' guide to the stop signal paradigm. In D. Dagenbach and T.H. Carr, editors, <i>Inhibitory processes in attention, memory, and language</i> , pages 189–239. Academic Press, San Diego, 1994.	939
877		940
878	8. F. Verbruggen and G.D. Logan. Response inhibition in the stop-signal paradigm. <i>Trends in Cognitive Sciences</i> , 12:418–424, 2008. http://doi.org/10.1016/j.tics.2008.07.005 .	941
879	9. D. Matzke, F. Verbruggen, and G.D. Logan. The stop-signal paradigm. In E.J. Wagenmakers, editor, <i>Stevens' Handbook of Experimental Psychology and Cognitive Neuroscience: Methodology</i> , volume 4. John Wiley & Sons, 4th edition, in press.	942
880		943
881	10. R. Carpenter and I. Noorani. Preface: Movement suppression: brain mechanisms for stopping and stillness. volume 372 of <i>Philosophical Transactions of the Royal Society B</i> . The Royal Society Publishing, 2017. 10.1098/rstb.2016.0542.	944
882	11. G.D. Logan and W.B. Cowan. On the ability to inhibit thought and action: a theory of an act of control. <i>Psychological Review</i> , 91(3):295–327, 1984.	945
883	12. J.D. Schall, T.J. Palmeri, and G.D. Logan. Models of inhibitory control. <i>Philosophical Transactions of the Royal Society of London B</i> , 372(20160193), 2017. http://dx.doi.org/10.1098/rstb.2016.0193 .	946
884	13. D.P. Hanes and J.D. Schall. Countermanding saccades in macaque. <i>Visual Neuroscience</i> , 12:929–937, 1995.	947
885	14. D.P. Hanes, W.F. Patterson, and J.D. Schall. Role of frontal eye field in countermanding saccades: visual, movement and fixation activity. <i>Journal of Neurophysiology</i> , 79:817–834, 1998.	948
886	15. M. Paré and D.P. Hanes. Controlled movement processing: superior colliculus activity associated with countermanded saccades. <i>Journal of Neuroscience</i> , 23:6480–6489, 2003.	949
887	16. J.W. Brown, D.P. Hanes, J.D. Schall, and V. Stuphorn. Relation of frontal eye field activity to saccade initiation during a countermanding task. <i>Experimental Brain Research</i> , 190:135–151, 2008. DOI 10.1007/s00221-008-1455-0.	950
888	17. L. Boucher, T.J. Palmeri, G.D. Logan, and J.D. Schall. Inhibitory control in mind and brain: an interactive race model of countermanding saccades. <i>Psychological Review</i> , 114(2):376–397, 2007.	951
889	18. J.D. Schall and D.C. Godlove. Current advances and pressing problems in studies of stopping. <i>Current Opinion in Neurobiology</i> , 22:1012–1021, 2012.	952
890	19. D.P. Hanes and J.D. Schall. Neural control of voluntary movement initiation. <i>Science</i> , 274:427–430, 1996.	953
891	20. G.D. Logan, M. Yamaguchi, J.D. Schall, and T.J. Palmeri. Inhibitory control in mind and brain 2.0: Blocked-input models of saccadic countermanding on the ability to inhibit thought and action: General and special theories of an act of control. <i>Psychological Review</i> , 122:115–147, 2015.	954
892	21. C.C. Lo, L. Boucher, M. Paré, J.D. Schall, and X.J. Wang. Proactive inhibitory control and attractor dynamics in countermanding action: a spiking neural circuit model. <i>Journal of Neuroscience</i> , 29:9059–9071, 2009.	955
893	22. R. B. Nelsen. <i>An introduction to copulas</i> , volume 139 of <i>Lecture Notes in Statistics</i> . Springer-Verlag, New York, NY, 2nd edition, 2006.	956
894	23. M. Denuit and J. Dhaene. Simple characterizations of comonotonicity and countermonotonicity by extremal correlations. <i>Belgian Actuarial Bulletin</i> , 3(1):22–27, 2003.	957
895	24. P.G. Bissett and G.D. Logan. Selective stopping? Maybe not. <i>Journal of Experimental Psychology: General</i> , 143(1):455–472, 2014.	958
896	25. H. Colonius. A note on the stop-signal paradigm, or how to observe the unobservable. <i>Psychological Review</i> , 97(2):309–312, 1990.	959
897	26. G.P.H. Band, M.W. van der Molen, and G.D. Logan. Horse-race model simulations of the stop-signal procedure. <i>Acta Psychologica</i> , 112:105–142, 2003.	960
898	27. D. Matzke, C.V. Dolan, G.D. Logan, S.D. Brown, and E.-J. Wagenmakers. Bayesian parametric estimation of stop-signal reaction time distributions. <i>Journal of Experimental Psychology: General</i> , 142(4):1047–1073, 2013.	961
899		962
900	Figure caption for Figure 1. The “fan” effect: all signal-response RT distributions $F_{sr}(t t_d)$ are strictly ordered by delay (t_d) from left to right, for $t_d = 10, 50, 100, 150$ [ms], converging toward no-stop signal distribution $F_{go}(t)$ (rightmost curve) for $t_d \rightarrow \infty$, for exponential distributions with rate parameters $\lambda_{go} = .01$ and $\lambda_{stop} = .02$; PND model curves were obtained by simulation (see Methods); dashed: IND model; solid: PND model.	963
901		964
902		965
903		966
904		967
905		968
906		969
907		970
908		971
909		972
910		973
911		974
912		975
913		976
914		977
915		978
916		979
917		980
918		981
919		982
920		983
921		984
922		985
923		986
924		987
925		988
926		989
927		990
928		991
929		992
930		

993
994
995
996
997
998
999
1000
1001
1002
1003
1004
1005
1006
1007
1008
1009
1010
1011
1012
1013
1014
1015
1016
1017
1018
1019
1020
1021
1022
1023
1024
1025
1026
1027
1028
1029
1030
1031
1032
1033
1034
1035
1036
1037
1038
1039
1040
1041
1042
1043
1044
1045
1046
1047
1048
1049
1050
1051
1052
1053
1054

1055
1056
1057
1058
1059
1060
1061
1062
1063
1064
1065
1066
1067
1068
1069
1070
1071
1072
1073
1074
1075
1076
1077
1078
1079
1080
1081
1082
1083
1084
1085
1086
1087
1088
1089
1090
1091
1092
1093
1094
1095
1096
1097
1098
1099
1100
1101
1102
1103
1104
1105
1106
1107
1108
1109
1110
1111
1112
1113
1114
1115
1116

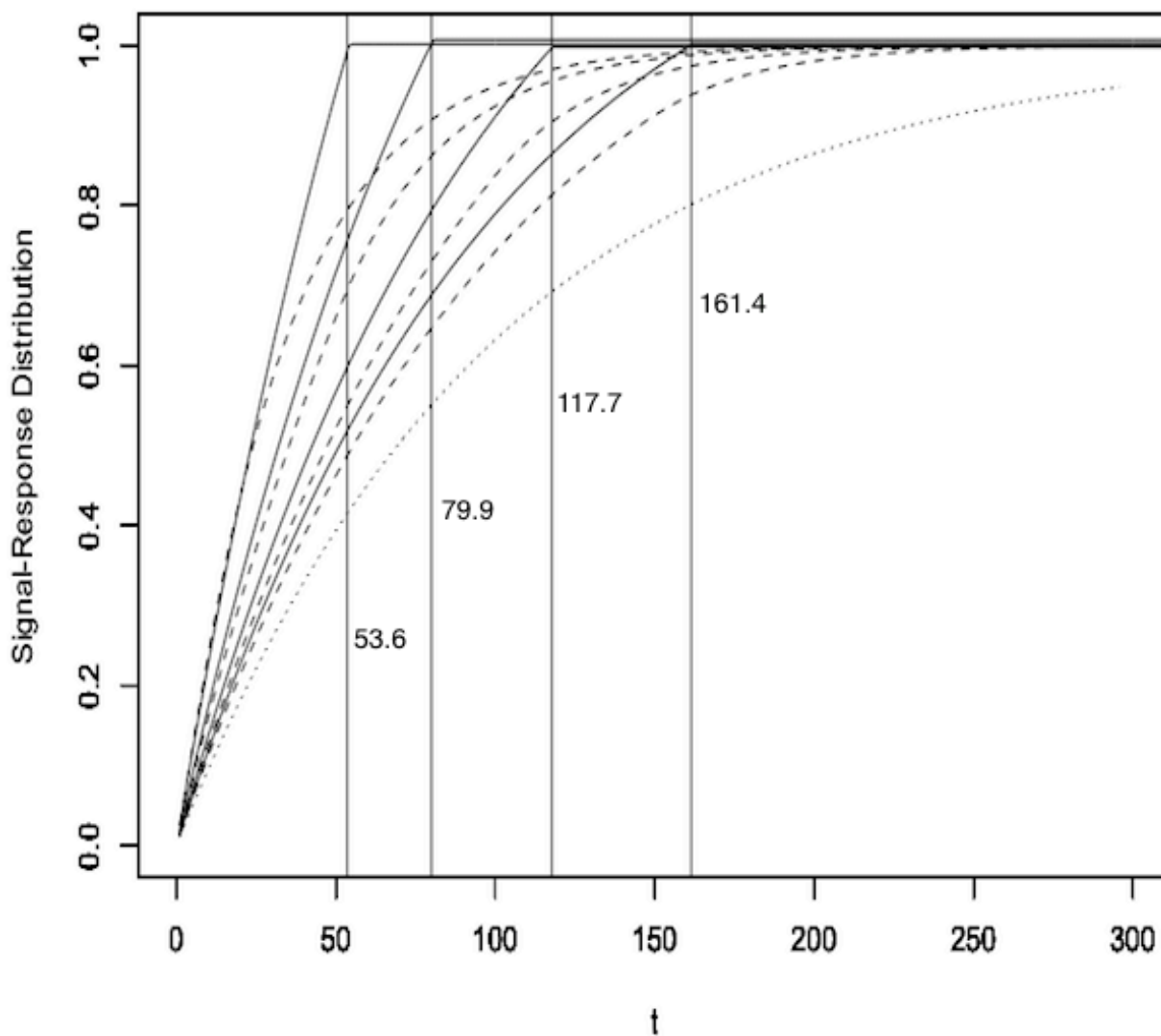


Fig. 1